

Cycle Expansions for Intermittent Maps

Roberto ARTUSO,^{1,*}) Predrag CVITANOVIĆ^{2,**}) and Gregor TANNER^{3,***})

¹*Dipartimento di Scienze Chimiche, Fisiche e Matematiche,
Università dell'Insubria and I.N.F.M.,*

Sezione di Como, Via Valleggio 11, 22100 Como, Italy

²*Center for Nonlinear Science, School of Physics, Georgia Institute of Technology,
Atlanta, GA 30332-0430, USA*

³*Quantum Information Processing Group, Hewlett-Packard Laboratories,
Bristol BS34 8QP, UK*

In a generic dynamical system chaos and regular motion coexist side by side, in different parts of the phase space. The border between these, where trajectories are neither unstable nor stable but of marginal stability, manifests itself through intermittency, dynamics where long periods of nearly regular motions are interrupted by irregular chaotic bursts. We discuss the Perron-Frobenius operator formalism for such systems, and show by means of a 1-dimensional intermittent map that intermittency induces branch cuts in dynamical zeta functions. Marginality leads to long-time dynamical correlations, in contrast to the exponentially fast decorrelations of purely chaotic dynamics. We apply the periodic orbit theory to quantitative characterization of the associated power-law decays.

§1. Introduction

In fluid dynamics one often observes long periods of regular dynamics (laminar phases) interrupted by irregular chaotic bursts, with the distribution of laminar phase intervals well described by a power law. This phenomenon is called *intermittency*,^{1),2)} and it is a very general aspect of dynamics, a shadow cast by non-hyperbolic and marginally stable phase space regions. Complete hyperbolicity is indeed the exception rather than the rule: almost any dynamical system of interest exhibits a mixed phase space where islands of stability or regular regions coexist with hyperbolic regions with dynamics mixing exponentially fast. The trajectories on the border between chaos and regular dynamics are marginally stable, and trajectories from chaotic regions which come close to marginally stable regions can stay 'glued' there for arbitrarily long times. These intervals of regular motion are interrupted by irregular bursts as the trajectory is re-injected into the chaotic part of the phase space. How the trajectories are precisely 'glued' to the marginally stable region is often hard to describe. What coarsely looks like a border of an island in a Hamiltonian system with a mixed phase space, will under magnification dissolve into infinities of island chains of decreasing sizes and cantori.³⁾

The existence of marginal or nearly marginal orbits is due to incomplete intersections of stable and unstable manifolds in a Smale horseshoe type dynamics. Following

*) E-mail: Roberto.Artuso@uninsubria.it

**) E-mail: Predrag.Cvitanovic@physics.gatech.edu

***) On leave from School of Mathematical Sciences, University of Nottingham, UK.

E-mail: Gregor.Tanner@nottingham.ac.uk

the stretching and folding of the invariant manifolds in time one will inevitably find phase space points at which the stable and unstable manifolds are almost or exactly tangential to each other, implying non-exponential separation of nearby points in phase space or, in other words, marginal stability.

How to deal with the full complexity of a typical Hamiltonian system with a mixed phase space is a very difficult and still open problem. Nevertheless, it is possible to learn quite a bit about intermittency by considering rather simple examples. Here we shall restrict our considerations to 1-dimensional maps which in the neighborhood of a single marginally stable fixed point at $x=0$ take the form

$$x \mapsto f(x) \sim x + cx^{1+s} \quad (1.1)$$

for $x \rightarrow 0$ and are expanding everywhere else. Such a map may allow for escape or the dynamics may be bounded, like the Farey map

$$x \mapsto f(x) = \begin{cases} f_0(x) = x/(1-x) & x \in \mathcal{M}_0 = [0, 1/2] \\ f_1(x) = (1-x)/x & x \in \mathcal{M}_1 = (1/2, 1] \end{cases}, \quad (1.2)$$

which has been studied intensively in connection with continued fraction expansions and circle maps.^{4)–11)}

The dynamics of the Farey map, which is of the form (1.1) with $s = 1$, is compared to that of the hyperbolic, piecewise linear tent map

$$x \mapsto f(x) = \begin{cases} f_0(x) = 2x & x \in \mathcal{M}_0 = [0, 1/2] \\ f_1(x) = 2(1-x) & x \in \mathcal{M}_1 = (1/2, 1] \end{cases} \quad (1.3)$$

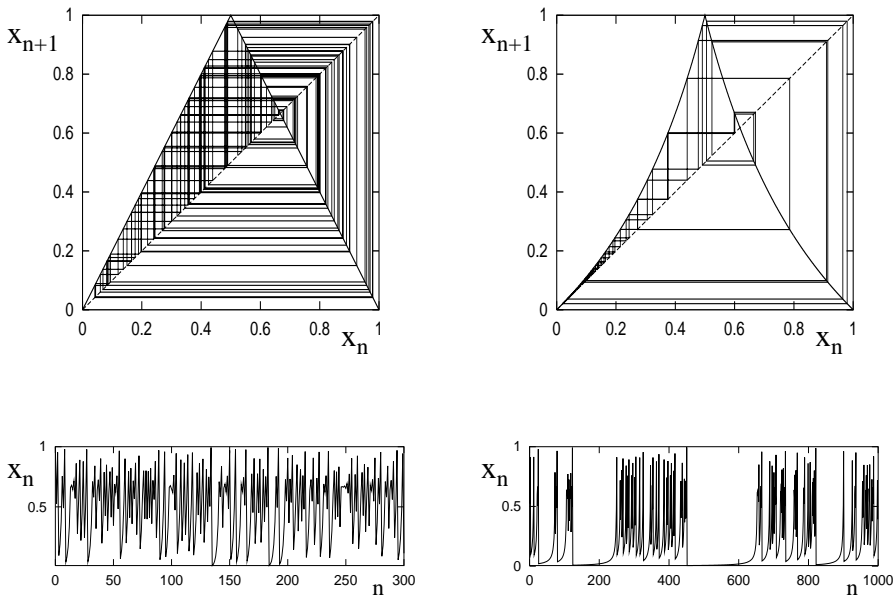


Fig. 1. (a) A tent map trajectory. (b) A Farey map trajectory.

in Fig. 1. In sharp contrast to the uniformly chaotic trajectory of the tent map, the Farey map trajectory alternates intermittently between slow regular motion close to the marginally stable fixed point, and chaotic bursts. The presence of marginal stability has striking dynamical consequences: correlation decay may exhibit long range power law asymptotic behavior and diffusion processes can assume anomalous character whereas escape from a repeller may be algebraic rather than exponential. In quantum mechanical systems linked to a classical deterministic dynamics via periodic orbit trace formula, intermittency can be shown to lead to localisation and quasi-regular eigenfunctions.^{12)–14)}

The Ruelle thermodynamical formalism^{15)–17)} relates dynamical averages to the spectral properties of the Perron-Frobenius operator or generalizations thereof, the Ruelle-Araki operators. For a 1-dimensional map a Perron-Frobenius operator relates the density at current time to the density at the previous time step:

$$\rho_{n+1}(x) = \mathcal{L}[\rho_n](x) = \int dy \delta(x - f(y)) \rho_n(y) = \sum_{f(y)=x} |f'(y)|^{-1} \rho_n(y). \quad (1.4)$$

Here we shall show how the method of cycle expansions may be applied to the calculation of spectra of Perron-Frobenius operators in the presence of marginally stable orbits. We start in §2.1 by recapitulating the theory for hyperbolic maps, and introduce dynamical zeta functions, spectral determinants, and their cycle expansions. In §2.2 we describe Perron-Frobenius operators in the presence of isolated marginally stable fixed points and introduce the induced map of an intermittent map. The core of the paper is §3; we explain how marginally stable orbits are incorporated in cycle expansions. In order to gain some appreciation for the difficulties lying ahead, we start in §3.1 by studying a piecewise linear map which follows the scaling (1.1) in the neighborhood of a fixed point, show that the dynamical zeta function has a branch cut, and extract from this cut the power law that characterizes the escape from the repeller.

Such branch cuts are typical also for smooth intermittent maps with isolated marginally stable fixed points and cycles. In §4 we discuss higher order curvature corrections required by their cycle expansions. The knowledge of the type of singularity one encounters for such systems enables us to construct the resummation method presented in §4.1. Analytic continuations of dynamical zeta functions in terms of their integral representations are discussed in §4.2.

§2. Perron-Frobenius operators and cycle expansions

Even though the operator formalism is not the focus of this paper, it is instructive to review it here as it sheds light on the cycle expansion approach pursued later. Briefly, when a dynamical system is uniformly hyperbolic and its symbolic dynamics is a subshift of finite type (a complete Smale horseshoe), spectral determinants of the associated evolution operators (like the Perron-Frobenius operator (1.4)) are entire and their spectra are discrete,¹⁸⁾ very much like the bound spectra of quantum, electrodynamic and elastodynamic systems. However, if either the requirement of

hyperbolicity, or of the finite subshift, or both are not fulfilled, the spectral determinant is no longer an entire function, with delicate consequences for the spectra of evolution operators.^{17), 19)}

We are far from having a global theory for non-hyperbolic dynamics; partial answers can, however, be given relating isolated features in the dynamics to spectral properties of the Perron-Frobenius operator. We will focus on a special case of non-hyperbolicity in what follows, that is, intermittent maps with complete symbolic dynamics and a single marginal fixed point. For intermittent dynamics where the symbolic dynamics is either not known, or cannot be finitely specified, a good practical method is the *stability ordered* cycle expansions.²⁰⁾ Alternatively, one can make use of statistical methods developed by Dahlqvist^{21), 22)} in which spectral determinants are approximately described in terms of probability distributions for the return time to the non-hyperbolic region.

Another example of non-hyperbolicity in the finite subshift setting is the Ulam map or logistic map $x \rightarrow 4x(1-x)$, with strongly contracting non-hyperbolic critical point $x_c = 1/2$. The Ulam map is conjugate to the tent map and this conjugacy fails only at the leftmost fixed point, the forward image of the critical point. It was shown in Ref. 9) that for maps, such as the “skew” Ulam map which cannot be conjugated to a tent map, the spectrum can be obtained by dividing out from the spectral determinant the fixed point that the critical point iterates to.

A similar technique needs to be employed when dealing with intermittency. As will be discussed later, marginally stable cycles are again factored out from the spectral determinant leading in this case, however, to a whole sub-determinant related to the dynamics close to the marginally stable point. The corresponding operator is (as can be shown by explicit conjugation) equivalent to free translation with a continuous spectrum, just as it is in quantum scattering where asymptotic states are also translation invariant. What remains of the factored spectral determinant can be interpreted as a spectral determinant of another dynamical system, the spectral determinant of a purely hyperbolic *induced map*.

2.1. The hyperbolic case — a review

In what follows we shall illustrate the key techniques by considering the dynamics of 1-dimensional hyperbolic maps $x \mapsto f(x)$ on the unit interval $\mathcal{M} = [0, 1]$ with two piecewise-analytic monotone branches

$$f(x) = \begin{cases} f_0(x) & x \in \mathcal{M}_0 = [0, a] \\ f_1(x) & x \in \mathcal{M}_1 = (b, 1] \end{cases} . \quad (2.1)$$

The two branches are assumed complete, $f_0(\mathcal{M}_0) = f_1(\mathcal{M}_1) = \mathcal{M}$. Such a map allows for escape if $a < b$, and the dynamics is bounded to the unit interval if $a = b$. Its symbolic dynamics is the full binary shift, with a 1-to-1 mapping between admissible orbits and all possible infinite binary itineraries. A map is hyperbolic if the stability exponents of all periodic orbits are strictly positive

$$\frac{1}{n_p} \ln |A_p| = \frac{1}{n_p} \sum_{i=1}^{n_p} \ln |f'(x_i)| \geq c > 0, \quad (2.2)$$

where the sum is over the cycle points x_i along the cycle p . In this case a well established theory exists,^{15), 18)} and it can be shown that the Perron-Frobenius operators have discrete spectra $\{\lambda_0, \lambda_1, \lambda_2 \dots\}$ when acting on a suitable space of real analytic functions. The method of *cycle expansions*^{23), 24), 17)} is often an efficient method of computing the spectrum. It makes use of the fact that the trace of the Perron-Frobenius operator can be written in terms of the periodic orbits of the map,

$$\mathrm{tr} \mathcal{L}^n = \sum_{\alpha} \lambda_{\alpha}^n = \int_0^1 dx \delta(x - f^n(x)) = \sum_i^{(n)} \frac{1}{|1 - A_i|}, \quad (2.3)$$

where the sum is taken over all periodic points of period n . The spectral determinant of \mathcal{L} is related to the traces by the cumulant expansion,¹⁷⁾

$$\begin{aligned} \det(1 - z\mathcal{L}) &= 1 - z \mathrm{tr} \mathcal{L} - \frac{1}{2} z^2 [\mathrm{tr} \mathcal{L}^2 - (\mathrm{tr} \mathcal{L})^2] - \dots \\ &= \prod_{k=0}^{\infty} \prod_p \left(1 - \frac{z^{np}}{|A_p| A_p^k} \right) = \prod_{k=0}^{\infty} \zeta_k^{-1}(z), \end{aligned} \quad (2.4)$$

where the product runs over all prime periodic orbits (repetitions excluded) of periods n_p . For hyperbolic maps with complete binary symbolic dynamics, the spectral determinant is an entire function^{15), 18)} whose zeros $\{z_0, z_1, z_2, \dots\}$ are related to the eigenvalues of the Perron-Frobenius operator via $\lambda_{\alpha} = z_{\alpha}^{-1}$.

A quantity easily accessible to experiment and numerical calculations is the survival probability $\hat{\Gamma}_n$, that is the fraction of phase space which remains within the phase space volume \mathcal{M} (with $\mathcal{M} = [0, 1]$ for the map (2.1)) for at least n iterations

$$\hat{\Gamma}_n = \frac{1}{|\mathcal{M}|} \sum_i^{(n)} |\mathcal{M}_i|. \quad (2.5)$$

Each surviving interval \mathcal{M}_i contains a periodic point $x_i \in \mathcal{M}_i$ belonging to a prime cycle p or its r th repeat, of total period $rn_p = n$. For hyperbolic maps their size can be asymptotically bounded from below and above in terms of the stabilities of that orbit,

$$\mathcal{C}_1 \frac{1}{|A_p|} < \frac{|\mathcal{M}_i|}{|\mathcal{M}|} < \mathcal{C}_2 \frac{1}{|A_p|}, \quad (2.6)$$

with $\mathcal{C}_1, \mathcal{C}_2$ independent of p . The asymptotic behavior of $\hat{\Gamma}_n$ is thus captured by the periodic orbit sum

$$\hat{\Gamma}_n \sim \Gamma_n = \sum_i^{(n)} \frac{1}{|A_i|}. \quad (2.7)$$

For strictly hyperbolic maps this survival probability falls off exponentially with n in the large n limit. The periodic orbit sum (2.7) can be rewritten in terms of $1/\zeta_0$ defined in (2.4),

$$\Gamma_n = \frac{1}{2\pi i} \oint_{\gamma_r^-} z^{-n} \left(\frac{d}{dz} \log \zeta_0^{-1}(z) \right) dz, \quad (2.8)$$

where the contour encircles the origin in the clockwise direction and lies inside the unit circle $|z| = 1$. The dynamical zeta function $1/\zeta_0$ can be written as a convergent product over periodic orbits in this region, integrals and sums can be interchanged, and the formula (2.7) is recovered after evaluating the integrals term by term by Cauchy integration. For hyperbolic maps, cycle expansions (discussed in more detail below) provide an analytic extension of the dynamical zeta function beyond the leading zero; we may then deform the original contour into a larger circle with radius R which encircles both poles and zeros of $1/\zeta_0$. Residue calculus turns this into a sum over the zeros z_α and poles z_β of the dynamical zeta function,

$$\Gamma_n = \sum_{|z_\alpha| < R} \frac{1}{z_\alpha^n} - \sum_{|z_\beta| < R} \frac{1}{z_\beta^n} + \frac{1}{2\pi i} \oint_{\gamma_R^-} dz z^{-n} \frac{d}{dz} \log \zeta_0^{-1}, \quad (2.9)$$

where the last term gives a contribution from a large circle γ_R^- . We thus find exponential decay of Γ_n dominated in general by the leading zero z_0 of $1/\zeta_0(z)$. We expect $z_0 = 1$ for bounded dynamics and $|z_0| > 1$ for maps which allow for escape.

The all important caveat here is whether one is able to construct an analytic continuation of $1/\zeta_0(z)$ for $|z| > |z_0|$. For systems with a complete symbolic dynamics with finite alphabet the method of cycle expansions,⁹⁾ with cycles and products of cycles (pseudo-cycles) ordered by their total period, has been demonstrated to work very well. For maps with a binary symbolic dynamics one has

$$\begin{aligned} 1/\zeta_0(z) &= \prod_p \left(1 - \frac{z^{n_p}}{|A_p|} \right) = 1 - \sum_{n=1}^{\infty} c_n \\ &= 1 - z \left[\frac{1}{|A_0|} + \frac{1}{|A_1|} \right] - z^2 \left[\frac{1}{|A_{01}|} - \frac{1}{|A_0 A_1|} \right] - z^3 [\dots] - \dots \end{aligned} \quad (2.10)$$

Here the c_1 term, the *fundamental* term, includes all unbalanced, not shadowed cycles. For the higher terms, called *curvature* corrections, large cancellations between cycles and pseudo-cycles that shadow them take place.^{9), 17)}

For a piecewise linear map like the tent map (1.3) with $|A_p| = 2^{n_p}$ for all periodic orbits of length n_p , contributions from cycles and pseudo-cycles cancel exactly and the curvature contributions are identically zero. The dynamical zeta function thus has the form

$$1/\zeta_0(z) = 1 - z \quad (2.11)$$

and vanishes at $z_0 = 1$, as expected. In this case the complete spectrum of the Perron-Frobenius operator $\{\lambda_0, \lambda_1, \lambda_2, \dots\}$ can easily be deduced from a cycle expansion of higher order dynamical zeta functions $1/\zeta_k(z)$; one obtains $\lambda_\alpha = z_\alpha^{-1} = 1/2^{2\alpha}$ for $\alpha = 0, 1, 2, \dots$.

2.2. The intermittent case and the induced map

For intermittent maps of the form (1.1) the trace and determinant formulas (2.3), (2.4) have no meaning as they stand; the periodic orbit stabilities can be arbitrary close or equal to 1, and that renders the formulas singular. A spectral analysis of

the Perron-Frobenius operator is now much subtler than in the hyperbolic case. In this section we briefly sketch the main ideas behind the recent breakthroughs in the spectral analysis for intermittent maps^{25)–28)} which establish that the Perron-Frobenius operator has a continuous spectrum $\sigma_c = [0, 1]$, and a pure point spectrum consisting of isolated eigenvalues of finite multiplicity. Due to the symmetry of the map, in this case zero is an eigenvalue of infinite multiplicity. We shall return to dynamical zeta functions and spectral determinants in §3.2 and will show there that marginal orbits induce branch cuts in zeta functions which are related to the continuous part of the spectrum.

The starting point for a rigorous analysis is the precise specification of the function space that the Perron-Frobenius operator acts on. This requires a level of analysis that lies beyond the scope of this paper: in particular, one needs to prove that \mathcal{L} maps this function space into itself. In what follows we will only give the key steps of the operator approach, which will be instructive later when discussing cycle expansions, without attempting to give details of the proofs.

The basic idea is to separate the intermittent part of the dynamics from the chaotic dynamics. For clarity, we shall illustrate the method using the Farey map (1.2) as an example.^{27), 28)} Denote by $F_i(x)$, $i \in \{0, 1\}$ the inverse of the branch f_i with $F_0(x) = x/(x+1)$ and $F_1(x) = 1/(x+1)$. F_i maps the unit interval \mathcal{M} into \mathcal{M}_i , the interval supporting f_i . For the Farey map, the Perron-Frobenius operator (1.4) acts on the two branches as

$$\begin{aligned} \mathcal{L} &= \mathcal{L}_0 + \mathcal{L}_1, \\ \mathcal{L}_0[\rho](x) &= \frac{1}{(1+x)^2} \rho\left(\frac{x}{x+1}\right), \quad \mathcal{L}_1[\rho](x) = \frac{1}{(1+x)^2} \rho\left(\frac{1}{x+1}\right). \end{aligned} \quad (2.12)$$

We focus on the intermittent behavior of the 0-branch by formally factoring it out

$$(1 - z\mathcal{L}) = (1 - \hat{\mathcal{L}}(z)) \cdot (1 - z\mathcal{L}_0). \quad (2.13)$$

Expanding

$$(1 - \hat{\mathcal{L}}(z)) = (1 - z\mathcal{L}_0 - z\mathcal{L}_1) \frac{1}{1 - z\mathcal{L}_0} = 1 - z\mathcal{L}_1 \frac{1}{1 - z\mathcal{L}_0}$$

as a geometric series yields a formula for $\hat{\mathcal{L}}$:

$$\hat{\mathcal{L}}(z) = \sum_{m=1}^{\infty} z^m \mathcal{L}_1 \mathcal{L}_0^{m-1}. \quad (2.14)$$

Loosely speaking, the partial Perron-Frobenius operator \mathcal{L}_0 in the decomposition (2.13) is responsible for the continuous part of the spectrum, a new feature specific to intermittent dynamics, while $\hat{\mathcal{L}}$ adds isolated eigenvalues.

The operator \mathcal{L}_0 is conjugated to the shift operator $S[\varphi](x) = \varphi(1+x)$ under the transformation $\rho(x) = \mathcal{C}[\varphi](x) = \varphi(f_1(x))$. The shift operator has a continuous spectrum $\sigma_c = [0, 1]$ on a function space of analytic functions obtained by a generalized Laplace transform

$$\varphi(x) = \mathcal{F}[\psi](x) = \frac{1}{x^2} \int_0^{\infty} d\mu(s) e^{-s/x} e^{-s} \psi(s)$$

acting on the space of square integrable functions $\psi \in L^2(\mathbb{R}_+, \mu)$ with $d\mu(s) = (e^s - 1)^{-1} s ds$.²⁷⁾ Similar relations are expected to hold in neighborhoods of marginally stable fixed points for general intermittent maps.²⁵⁾

It remains to understand the role of $\hat{\mathcal{L}}$. The meaning of the formal power series (2.14) is best grasped by setting $z = 1$: the operator

$$\hat{\mathcal{L}}(1) = \hat{\mathcal{L}} = \sum_{m=1}^{\infty} \mathcal{L}_1 \mathcal{L}_0^{m-1}$$

is the Perron-Frobenius operator for the map⁹⁾

$$\hat{f}(x) = \begin{cases} f_1(x) & x \in \mathcal{M}_1 \\ f_2(x) = f_1(f_0(x)) & x \in \mathcal{M}_2 = (q_2, q_1] \\ \vdots & \vdots \\ f_m(x) = f_1(f_0^{(m-1)}(x)) & x \in \mathcal{M}_m = (q_m, q_{m-1}] \\ \vdots & \vdots \end{cases}, \quad (2.15)$$

constructed from compositions of the initial 2-branch map f defined in (2.1). The interval boundaries q_n are successive preimages $f_0(q_n) = q_{n-1}$ of the rightmost point of \mathcal{M}_0 , that is, $q_1 = 1/2$ for the Farey map or $q_1 = a$ in case of the map (2.1). The map \hat{f} thus has an infinity of branches, taking care of all sequences of consecutive iterations of the left branch of f in a single step. The length of a cycle of \hat{f} thus equals the number of 1's in the binary itinerary of the original map f . For the Farey map the map (2.15) is the Gauss map of number theory¹⁰⁾

$$\hat{f}_{\text{Gauss}}(x) = \left\{ \frac{1}{x} \right\}, \quad x \in (0, 1],$$

where $\{\dots\}$ denotes the fractional part. This map is related by conjugacy to the *induced map* of Refs. 29), 30), the first return map on interval $[1/2, 1]$. The key issue is that the induced map is hyperbolic, so the operator $\hat{\mathcal{L}}$ adds only isolated eigenvalues to the spectrum.

Now, factoring out parts of the spectral determinant implicit in (2.13) does not necessarily make sense. If the spectral determinant is an entire function, as it is for hyperbolic maps, this merely introduces singularities in the remainder term and the spectrum of \mathcal{L}_0 may have little in common with the spectrum of the full Perron-Frobenius operator \mathcal{L} . Things are, however, different for intermittent maps. The determinant $\det(1 - \hat{\mathcal{L}}(z))$ is analytic in $\mathbb{C} - [1, \infty)$, with a branch cut along the real line $[1, \infty)$, and can be analytically continued through this branch cut, albeit onto different Riemann sheets. Hence $\sigma_c = [0, 1]$ is part of the spectrum of the full operator \mathcal{L} , while the rest of the spectrum of \mathcal{L} is discrete and can be deduced from $\hat{\mathcal{L}}$. From (2.13) it follows now that z^{-1} is an eigenvalue of \mathcal{L} if 1 is an eigenvalue of $\hat{\mathcal{L}}(z)$.

Let us finally return to the spectral determinant of $\hat{\mathcal{L}}$. The dynamics of f and \hat{f} are equivalent apart from singling out the fixed point at $x = 0$. As a consequence,

very little changes when writing the spectral determinant (2.4) for $\hat{\mathcal{L}}(z)$ in terms of periodic orbits except for taking out the marginal fixed point, that is,

$$\det \left(1 - \hat{\mathcal{L}}(z) \right) = \prod_{k=0}^{\infty} \prod_{p \neq 0} \left(1 - \frac{z^{n_p}}{|A_p| A_p^k} \right), \quad (2.16)$$

where n_p is again the length of the periodic orbit with respect to the original map f . That something more profound is happening becomes clear when we consider the first few terms in the cumulant expansion of the spectral determinant Eq. (2.4),

$$\det \left(1 - \hat{\mathcal{L}}(z) \right) = 1 - \text{tr} \hat{\mathcal{L}}(z) - \dots = 1 - \sum_{m=1}^{\infty} \frac{z^m}{|1 - A_{10^{m-1}}|} - \dots \quad (2.17)$$

The infinite sum over orbits 10^{m-1} reflects the fact that the induced map has infinitely many fixed points.

§3. Periodic orbit expansions for intermittent maps

In order to get to know the kind of problems which arise when studying dynamical zeta functions in the presence of marginal stability we shall train on a carefully crafted piecewise linear map first, and return to the case of smooth intermittent maps in §4.

3.1. A piecewise linear toy map

The tent map (1.3) is an idealized example of a hyperbolic map. To construct a piecewise linear analogue for intermittency, we start from the induced map (2.15), linear in each branch. ³¹⁾

We take the right branch in (2.1) expanding and linear:

$$f_1(x) = \frac{1}{1-b}(x-b) \quad \text{for } x \in \mathcal{M}_1 = (b, 1].$$

The left branch f_0 of f is constructed in such a way that it will exhibit the intermittent behavior (1.1) near the origin. Motivated by the form of the induced map (2.15), we consider a monotonically decreasing sequence q_m of preimages of the rightmost point of f_0 in $\mathcal{M}_0 = [0, a]$, with $q_1 = a$ and $q_m \rightarrow 0$ as $m \rightarrow \infty$. This sequence defines a partition of the left interval \mathcal{M}_0 into an infinite number of monotonically decreasing intervals \mathcal{M}_m , $m \geq 2$ with

$$\mathcal{M}_m = (q_m, q_{m-1}] \quad \text{and} \quad \mathcal{M}_0 = \bigcup_{m=2}^{\infty} \mathcal{M}_m. \quad (3.1)$$

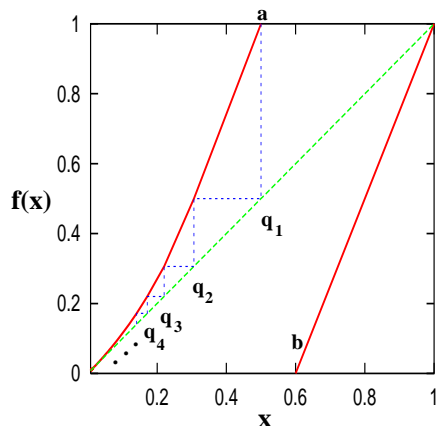


Fig. 2. A piecewise linear intermittent map of type (2.1) for intervals chosen according to (3.5) with $a = .5$, $b = .6$, $s = 1.0$

Conversely, any given monotone sequence $\{q_m\}$ defines a piecewise linear continuous map $f_0(x)$, with the slopes of the various linear segments given by

$$\begin{aligned} f'_1(x) &= \frac{1}{1-b} && \text{for } x \in \mathcal{M}_1, \\ f'_0(x) &= \frac{1-a}{|\mathcal{M}_2|} && \text{for } x \in \mathcal{M}_2, \\ f'_0(x) &= \frac{|\mathcal{M}_{m-1}|}{|\mathcal{M}_m|} && \text{for } x \in \mathcal{M}_m, \quad m \geq 3 \end{aligned} \quad (3.2)$$

with $|\mathcal{M}_m| = q_{m-1} - q_m$ for $m > 1$.

We have seen in (2.15) and (2.17) that the family of periodic orbits with itinerary 10^{m-1} plays a key role for intermittent maps of the form (1.1). An orbit 10^{m-1} enters the intervals $\mathcal{M}_1 \rightarrow \mathcal{M}_m \rightarrow \mathcal{M}_{m-1}, \dots \rightarrow \mathcal{M}_2$ successively and the family comes closer and closer to the marginally stable fixed point at $x = 0$ as $m \rightarrow \infty$. The stability of a cycle 10^{m-1} for $m \geq 2$ is proportional to the size of the interval closest to the marginal fixed point

$$A_{10^{m-1}} = f'_0(x_m) f'_0(x_{m-1}) \cdots f'_0(x_2) f'_1(x_1) = \frac{1}{|\mathcal{M}_m|} \frac{1-a}{1-b}, \quad (3.3)$$

with $x_i \in \mathcal{M}_i$.

A piecewise linear map of the form (2.1) is fixed by the sequence $\{q_m\}$. By choosing $q_m = 2^{-m}$, for example, we recover the uniformly hyperbolic Bernoulli shift map. An algebraically decaying sequence $\{q_m\}$

$$q_m \sim \frac{1}{m^{1/s}}, \quad |\mathcal{M}_m| \sim \frac{1}{m^{1+1/s}}, \quad (3.4)$$

yields an intermittent map of the form (3.1), with the asymptotic behavior controlled by the intermittency exponent s in (1.1). The stability eigenvalues of periodic orbit families approaching the marginally stable fixed point, such as the 10^{m-1} family in (3.3), grow in turn only algebraically (not exponentially) with the cycle length.

It may now seem natural to construct an intermittent toy map in terms of a partition $|\mathcal{M}_m| = 1/m^{1+1/s}$, that is, a partition which follows (3.4) exactly. Such a choice leads to a dynamical zeta function which can be written in terms of Jonquière functions (or polylogarithms).^{32), 33)} We shall, however, use the freedom in choosing the partition to make life as simple as possible later on, without losing the key intermittency features. Inspired by a bit of reverse engineering we fix the intermittent map intervals \mathcal{M}_m by

$$|\mathcal{M}_m| = \mathcal{C} \frac{\Gamma(m + \ell - 1/s - 1)}{\Gamma(m + \ell)} \quad \text{for } m \geq 2, \quad (3.5)$$

where $\Gamma(x)$ is the Gamma function, $\ell = [1/s]$ denotes the integer part of $1/s$, and the normalization constant \mathcal{C} is fixed by the full partition condition $\sum_{m=2}^{\infty} |\mathcal{M}_m| = q_1 = |\mathcal{M}_0|$, that is,

$$\mathcal{C} = |\mathcal{M}_0| \left[\sum_{m=\ell+1}^{\infty} \frac{\Gamma(m - 1/s)}{\Gamma(m + 1)} \right]^{-1}. \quad (3.6)$$

One easily verifies that the intervals decay asymptotically like $m^{-(1+1/s)}$ as required by the condition (3.4) using Stirling's formula for the Gamma function.

The point spectrum of f is given by the zeros of the spectral determinant (2.14) or the associated dynamical zeta functions. In order to find analytic continuations of the dynamical zeta function $1/\zeta_k$, we start by expanding the product as we did in (2.10).

Due to the absence of the fixed point 0, there are no pseudo-cycles that shadow cycles of the form 10^{m-1} , so the fundamental cycles are now the entire infinite family of cycles with itineraries of the form 10^{m-1} accumulating towards the marginal fixed point $\bar{0}$. As the $\bar{0}$ fixed point does not participate in the dynamics, we have to switch from the 2-letter $\{0, 1\}$ alphabet to the infinite alphabet $m = 10^{m-1}$ which labels the branches of the induced map (2.15). The admissible itineraries are now generated by all walks on the infinite Markov diagram⁹⁾ Fig. 3.

The piecewise linear form of the map which maps intervals \mathcal{M}_m exactly onto \mathcal{M}_{m-1} simplifies matters considerably: when expanding the zeta functions in the spectral determinant (2.16) all cycles which traverse the right branch at least twice are cancelled exactly by pseudo-cycles. The cycle expanded dynamical zeta functions depend thus only on the fundamental cycles and have the form

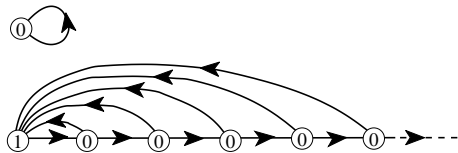


Fig. 3. Markov graph for the infinite alphabet $\{m = 10^{m-1}; \bar{0}, m \geq 1\}$ derived from full binary symbolic dynamics by separating out the $\bar{0}$ fixed point.

$$1/\zeta_k(z) = \prod_{p \neq 0} \left(1 - \frac{z^{n_p}}{|A_p|A_p^k} \right) = 1 - \sum_{m=1}^{\infty} \frac{z^m}{|A_{10^{m-1}}|A_{10^{m-1}}^k}. \quad (3.7)$$

To keep the discussion simple, we will restrict our considerations to $1/\zeta_0$. We obtain

$$1/\zeta_0(z) = 1 - (1-b)z - c \frac{1-b}{1-a} \sum_{m=2}^{\infty} \frac{\Gamma(m+\ell-1/s-1)}{\Gamma(m+\ell)} z^m. \quad (3.8)$$

The cycle expansion does not, however, lead to an analytic continuation here, despite the exact cancellation between cycles and pseudo-cycles, in contrast to the dynamical zeta function for the tent map (1.3). Due to the slow, algebraic decay of cycle weights, the sum (3.8) is divergent for $|z| > 1$. We shall now show that this behavior is due to a branch cut in $1/\zeta_k(z)$ along $[1, \infty)$.

3.2. Branch cuts in dynamical zeta functions due to intermittency

In order to analytically continue the sum (3.8) beyond $|z| \geq 1$ we make use of the following binomial identities valid for $\alpha = 1/s > 0$:

$$\alpha \text{ non-integer} \quad (1-z)^\alpha = \sum_{n=0}^{\infty} \frac{\Gamma(n-\alpha)}{\Gamma(-\alpha)\Gamma(n+1)} z^n,$$

$$\alpha \text{ integer} \quad (1-z)^\alpha \log(1-z) = \sum_{n=1}^{\alpha} (-1)^n c_n z^n + (-1)^{\alpha+1} \alpha! \sum_{n=\alpha+1}^{\infty} \frac{(n-\alpha-1)!}{n!} z^n,$$

$$\text{with } c_n = \binom{\alpha}{n} \sum_{k=0}^{n-1} \frac{1}{\alpha-k}. \quad (3.9)$$

For simplicity sake, we restrict the intermittency parameter to $1 \leq 1/s < 2$, that is the case $[1/s] = \ell = 1$. All that follows can easily be generalized to arbitrary $s > 0$ using (3.9). What once was a mystifying choice of interval widths (3.5) now pays off: the infinite sum (3.8) can be evaluated analytically,

$$\sum_{m=2}^{\infty} \frac{\Gamma(m-1/s)}{\Gamma(m+1)} z^m = \begin{cases} \Gamma(-\frac{1}{s}) [(1-z)^{1/s} - 1 + \frac{1}{s}z] & \text{for } 1 < 1/s < 2; \\ (1-z) \log(1-z) + z & \text{for } s = 1. \end{cases}$$

The normalization constant \mathcal{C} in (3.6) can be evaluated, and one obtains for $1 < 1/s < 2$:

$$1/\zeta_0(z) = 1 - (1-b)z - \frac{a}{1/s-1} \frac{1-b}{1-a} \left((1-z)^{1/s} - 1 + \frac{1}{s}z \right) \quad (3.10)$$

and for $s = 1$:

$$1/\zeta_0(z) = 1 - (1-b)z - a \frac{1-b}{1-a} ((1-z) \log(1-z) + z). \quad (3.11)$$

For general $s > 0$ one obtains

$$1/\zeta_0(z) = 1 - (1-b)z - \frac{a}{g_s(1)} \frac{1-b}{1-a} \frac{1}{z^{\ell-1}} \left((1-z)^{1/s} - g_s(z) \right) \quad (3.12)$$

for non-integer s with $\ell = [1/s]$ and

$$1/\zeta_0(z) = 1 - (1-b)z - \frac{a}{g_s(1)} \frac{1-b}{1-a} \frac{1}{z^{\ell-1}} \left((1-z)^\ell \log(1-z) - g_s(z) \right) \quad (3.13)$$

for $1/s = \ell$ integer; here, $g_s(z)$ are polynomials of order $\ell = [1/s]$ which can be deduced from (3.9). We see that the dynamical zeta function has a branch cut starting at $z = 1$ and running along the positive real axis. We find algebraic branch cuts for non integer intermittency exponents $1/s$ and logarithmic branch cuts for $1/s$, integer. We will see in §4 that branch cuts of that form are generic for 1-dimensional intermittent maps. In the next section, we will use these analytic expressions to calculate the escape from our toy map for $a < b$ in (2.1).

3.3. Escape rate

The fraction of survivors Γ_n defined in (2.5) have for hyperbolic maps been linked to $1/\zeta_0$ with the help of bounds given in (2.6). These bounds are no longer valid for intermittent maps. It turns out, however, that bounding survival probabilities strip by strip is a far too strict requirement for establishing the relation (2.7). In fact, a somewhat weaker bound can be established, linking the average size of intervals

along a periodic orbit to the stability of the periodic orbit for all but the interval \mathcal{M}_{0^n} . We can write this bound by averaging over each prime cycle p separately,

$$\mathcal{C}_1 \frac{1}{|\Lambda_p|} < \frac{1}{n_p} \sum_p \frac{|\mathcal{M}_p^{(n_p)}|}{|\mathcal{M}|} < \mathcal{C}_2 \frac{1}{|\Lambda_p|}, \quad (3.14)$$

for some positive constants $\mathcal{C}_1, \mathcal{C}_2$ independent of p . A proof, which relies on the hyperbolicity of the induced map, can be found in Ref. 34). Summing over all periodic orbits leads then again to (2.7) which is linked to $1/\zeta_0$ via the integral representation (2.8).

The path deformation to $|z| > 1$ that led to (2.9) requires more care here, as it must not cross the branch cut along $[1, \infty]$. When expanding the contour to large $|z|$ values, we have to deform it in such a way that it sandwiches the branch cut in anti-clockwise direction, see Fig. 4. Denoting the detour around the cut as γ_{cut} , we may write symbolically

$$\oint_{\gamma_r} = \sum_{\text{zeros}} - \sum_{\text{poles}} + \oint_{\gamma_R} + \oint_{\gamma_{\text{cut}}},$$

where the sums include only the zeros and the poles in the area enclosed by the contours.

Let us now go back to our intermittent toy map. The asymptotics of the survival probability of the map is governed by the behavior of the integrand $\frac{d}{dz} \log \zeta_0^{-1}$ in (2.8) at the branch point $z = 1$. We restrict ourselves again to the case $1 < 1/s < 2$ first and write the dynamical zeta function (3.10) in the form

$$1/\zeta_0(z) = a_0 + a_1(1-z) + b_0(1-z)^{1/s} \equiv G(1-z)$$

with

$$a_0 = \frac{b-a}{1-a}, \quad b_0 = \frac{a}{1-1/s} \frac{1-b}{1-a}.$$

Setting $u = 1 - z$, we need to evaluate

$$\frac{1}{2\pi i} \oint_{\gamma_{\text{cut}}} (1-u)^{-n} \frac{d}{du} \log G(u) du, \quad (3.15)$$

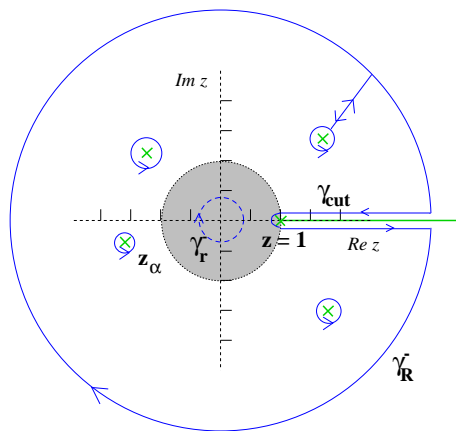


Fig. 4. The survival probability Γ_n calculated by contour integration; integrating (2.8) inside the domain of convergence $|z| < 1$ (shaded area) of $1/\zeta_0(z)$ in periodic orbit representation yields (2.7). A deformation of the contour γ_r^- (dashed line) to a larger circle γ_R^- (without crossing the branch cut) gives contributions from the poles and zeros (x) of $1/\zeta_0(z)$ between the two circles, as well as contributions from the integration along the branch cut γ_{cut} .

where γ_{cut} goes around the cut (that is, the negative u axis). Expanding the integrand $\frac{d}{du} \log G(u) = G'(u)/G(u)$ in powers of u and $u^{1/s}$ at $u = 0$, one obtains

$$\frac{d}{du} \log G(u) = \frac{a_1}{a_0} + \frac{1}{s} \frac{b_0}{a_0} u^{1/s-1} + O(u). \quad (3.16)$$

The integral along the cut may be evaluated using the general formula

$$\frac{1}{2\pi i} \oint_{\gamma_{\text{cut}}} u^\alpha (1-u)^{-n} du = \frac{\Gamma(n-\alpha-1)}{\Gamma(n)\Gamma(-\alpha)} \sim \frac{1}{n^{\alpha+1}} (1 + O(1/n)) \quad (3.17)$$

which can be obtained by deforming the contour back to a loop around the point $u = 1$, now in positive (anti-clockwise) direction. The contour integral then picks up the $(n-1)$ -st term in the Taylor expansion of the function u^α at $u = 1$, see (3.9).

Inserting (3.16) into (3.15) and using (3.17) we get the asymptotic result

$$\Gamma_n \sim \frac{b_0}{a_0} \frac{1}{s} \frac{1}{\Gamma(1-1/s)} \frac{1}{n^{1/s}} = \frac{a}{s-1} \frac{1-b}{b-a} \frac{1}{\Gamma(1-1/s)} \frac{1}{n^{1/s}}. \quad (3.18)$$

We see that, asymptotically, the escape from an intermittent repeller is described by power law decay rather than the exponential decay we are familiar with for hyperbolic maps. The zeros and poles of $1/\zeta_0$ give exponentially decreasing contributions, which may indeed be dominant over large time interval before the power law decay sets in for $n \rightarrow \infty$. A numerical simulation of the power-law escape from an intermittent repeller is shown in Fig. 5.

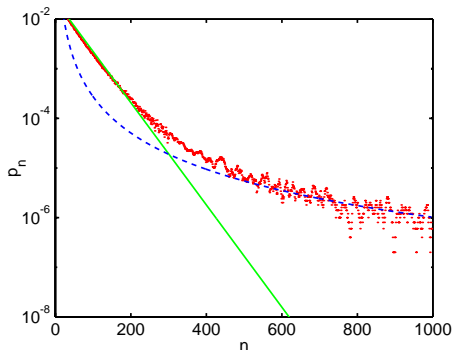


Fig. 5. The escape from an intermittent repeller typically starts out exponentially, controlled by the zeros close to the cut but beyond the branch point $z = 1$, as in Fig. 4, followed by a power law decay controlled by the type of the branch cut.

For general, non-integer $1/s > 0$, we write

$$1/\zeta_0(z) = A(u) + (u)^{1/s} B(u) \equiv G(u)$$

with $u = 1 - z$ and $A(u)$, $B(u)$ are functions analytic in a disc of radius 1 around $u = 0$. The leading terms in the Taylor series expansions of $A(u)$ and $B(u)$ are

$$a_0 = \frac{b-a}{1-a}, \quad b_0 = \frac{a}{g_s(1)} \frac{1-b}{1-a},$$

see (3.12). Expanding $\frac{d}{du} \log G(u)$ around $u = 0$, one again obtains leading order contributions according to (3.16) and the general result follows immediately using (3.17)

$$\Gamma_n \sim \frac{a}{sg_s(1)} \frac{1-b}{b-a} \frac{1}{\Gamma(1-1/s)} \frac{1}{n^{1/s}}. \quad (3.19)$$

Applying the same arguments for integer intermittency exponents $1/s = \ell$, one obtains

$$\Gamma_n \sim (-1)^{\ell+1} \frac{a}{sg_\ell(1)} \frac{1-b}{b-a} \frac{\ell!}{n^\ell}. \quad (3.20)$$

So far, we have considered the survival probability for a repeller, that is we assumed $a < b$. The formulas (3·19) and (3·20) do obviously not apply for the case $a = b$ of a bounded map. The coefficient $a_0 = (b - a)/(1 - a)$ in the series representation of $G(u)$ is zero and we need to take into account next leading terms in the expansion of the logarithmic derivative of $G(u)$ in (3·16). One obtains

$$\frac{d}{du} \log G(u) = \begin{cases} \frac{1}{u} (1 + O(u^{1/s-1})) & s < 1 \\ \frac{1}{u} (\frac{1}{s} + O(u^{1-1/s})) & s > 1 \end{cases} ,$$

where we assume $1/s$ non-integer for convenience. The survival probability is thus in leading order

$$\Gamma_n \sim \begin{cases} 1 + O(n^{1-1/s}) & s < 1 \\ 1/s + O(n^{1/s-1}) & s > 1 \end{cases} .$$

For $s < 1$, this is what we expect. There is no escape, so the survival probability is equal to 1, which we get as an asymptotic result here. The result for $s > 1$ is somewhat more worrying. It says that Γ_n defined as sum over the instabilities of the periodic orbits (2·7) does not tend to unity for large n . However, the case $s > 1$ is in many senses anomalous. For instance, the invariant density cannot be normalized.³⁵⁾ It is therefore not reasonable to expect that periodic orbit theories will work without complications.

§4. Smooth intermittent maps

Now we turn to the problem of constructing cycle expansions for general smooth 1-dimensional maps with a single isolated marginal fixed point. To keep the notation simple, we will consider two-branch maps with a complete binary symbolic dynamics as in (2·1). The necessary modifications for multi-branch maps with an isolated marginal fixed point are straightforward. We again assume that the behavior near the fixed point is given by (1·1). This implies that the stability of a family of cycles approaching the marginally stable orbit, for example the family 10^m , will increase only algebraically. Again we find for large m

$$\frac{1}{A_{10^m}} \sim \frac{1}{m^{1+1/s}} ,$$

where s denotes the intermittency exponent.

Zeta functions or spectral determinants in terms of products over cycles are formally identically to those of hyperbolic systems except for the omission of the marginal orbit 0, see (2·16). When considering cycle expansion as in §2.1, periodic orbit contributions from, for example, cycles with itinerary 10^m are unbalanced and we arrive at a cycle expansion in terms of infinitely many fundamental terms^{9), 13)} as for our toy map. This corresponds to moving from our binary symbolic dynamics to an infinite symbolic dynamics by making the identification

$$10^{m-1} \rightarrow m; \quad 10^{k-1}10^{m-1} \rightarrow km; \quad 10^{l-1}10^{k-1}10^{m-1} \rightarrow lkm; \dots ,$$

as in Table I. The topological length of the orbit is thus no longer determined by the iterations of the two-branch map f , but by the number of times the cycle reaches the

Table I. Infinite alphabet versus the original binary alphabet for the shortest periodic orbit families.

∞ - alphabet		binary alphabet				
		$m = 1$	$m = 2$	$m = 3$	$m = 4$	$m = 5$
1-cycle	m	1	10	100	1000	10000
2-cycle	km					
	$1m$	11	110	1100	11000	110000
	$2m$	101	0101	10100	101000	1010000
	$3m$	1001	10010	100100	1001000	10010000
	$4m$	10001	100010	1000100	10001000	100010000
3-cycle	lkm					
	$11m$	111	1110	11100	111000	1110000
	$12m$	1101	11010	110100	1101000	11010000
	$13m$	11001	110010	1100100	11001000	110010000
	$21m$	1011	10110	101100	1011000	10110000
	$22m$	10101	101010	1010100	10101000	101010000
	$23m$	101001	1010010	10100100	101001000	1010010000
	$31m$	10011	100110	1001100	10011000	100110000
	$32m$	100101	1001010	10010100	100101000	1001010000
	$33m$	1001001	10010010	100100100	1001001000	10010010000

right branch, that is, by the number of symbols 1 in the itinerary, or by the number of letters in the symbolic dynamics of the induced map \hat{f} of f .

For generic intermittent maps, curvature contributions in the cycle expanded zeta function will not vanish exactly as they do for our piecewise linear model. The most natural way to organize the cycle expansion in this case is to collect cycles and pseudo-cycles of the same topological length with respect to the infinite alphabet of the induced map. Denoting cycle weights in the new alphabet as $t_{km\dots} = t_{10^{k-1}10^{m-1}\dots}$, one obtains¹³⁾

$$\begin{aligned}
\zeta_0^{-1} &= \prod_{p \neq 0} (1 - t_p) = 1 - \sum_{n=1}^{\infty} c_n \\
&= 1 - \sum_{m=1}^{\infty} t_m - \sum_{k=1}^{\infty} \sum_{m=1}^{\infty} \frac{1}{2} (t_{km} - t_k t_m) \\
&\quad - \sum_{l=1}^{\infty} \sum_{k=1}^{\infty} \sum_{m=1}^{\infty} \left(\frac{1}{3} t_{lkm} - \frac{1}{2} t_{lk} t_m + \frac{1}{6} t_l t_k t_m \right) - \sum_{j=1}^{\infty} \sum_{l=1}^{\infty} \sum_{k=1}^{\infty} \sum_{m=1}^{\infty} \dots \quad (4.1)
\end{aligned}$$

with $t_p = z^{n_p} / |\Lambda_p|$ and n_p is the length of the binary itinerary. The first sum is the fundamental term, already noted in the cycle expansion (3.7) for the toy model. The curvature terms c_n for $n \geq 2$ are now n -fold infinite sums where the prefactors take care of double counting of prime cycles.

We consider the fundamental term first. For generic intermittent maps, we can not expect to obtain an analytic expression for infinite sums of the form

$$f(z) = \sum_{n=0}^{\infty} h_n z^n \quad (4.2)$$

with algebraically decreasing coefficients $h_n \sim n^{-(1/s+1)}$.

To evaluate the sum, we face the same problem as for our toy map: the power series diverges for $|z| > 1$, that is, exactly in the ‘interesting’ region where poles, zeros or branch cuts of the zeta function are to be expected. By carefully subtracting the asymptotic behavior with the help of (3·9), one can in general construct an analytic continuation of $f(z)$ around $z = 1$ of the form³⁶⁾

$$\begin{aligned} f(z) &\sim A(z) + B(z)(1-z)^{1/s}, & 1/s \notin \mathbb{N}, \\ f(z) &\sim A(z) + B(z)(1-z)^{1/s} \ln(1-z), & 1/s \in \mathbb{N}, \end{aligned} \quad (4.3)$$

where $A(z)$ and $B(z)$ are functions analytic in a disc around $z = 1$. From here we can derive the asymptotic behavior which coincides with the asymptotics obtained in (3·19) and (3·20), that is, the survival probability is in general given as

$$\Gamma_n \sim \frac{1}{n^{1/s}} \quad \text{for } n \rightarrow \infty \quad (4.4)$$

for 1-dimensional maps of the form (1·1). We have to work a bit harder if we want more detailed information like exponential precursors given by zeros or poles of the dynamical zeta function or higher order corrections. This information is buried in the functions $A(z)$ and $B(z)$ or more generally in the analytically continued zeta functions including curvature contributions. To get such an analytic continuation, one may follow two different strategies which we will sketch next.

4.1. Resummation

One way to get information about the zeta function near the branch cut is to derive the leading coefficients in the Taylor series of the functions $A(z)$ and $B(z)$ in (4·3) at $z = 1$. This can be done in principle, if the coefficients h_n in sums like (4·2) are known (as for our toy model). One then considers a resummation of the form^{36)–39)}

$$\sum_{j=0}^{\infty} h_j z^j = \sum_{j=0}^{\infty} a_j (1-z)^j + (1-z)^{1/s} \sum_{j=0}^{\infty} b_j (1-z)^j, \quad (4.5)$$

and the coefficients a_j and b_j are obtained in terms of the h_j by expanding $(1-z)^j$ and $(1-z)^{j+1/s}$ around $z = 0$ using (3·9), and equating the coefficients.

In practical calculations one often has only a finite number of coefficients h_j , $0 \leq j \leq n_N$, which may have been obtained by finding periodic orbits and their stabilities numerically. One can still design a resummation scheme for the computation of the coefficients a_j and b_j in (4·5). We replace the infinite sums in (4·5) by finite sums of increasing degrees n_a and n_b , and require that

$$\sum_{i=0}^{n_a} a_i (1-z)^i + (1-z)^{1/s} \sum_{i=0}^{n_b} b_i (1-z)^i = \sum_{i=0}^{n_N} h_i z^i + O(z^{n_N+1}) . \quad (4.6)$$

One proceeds again by expanding the right hand side around $z = 0$, skipping all powers z^{n_N+1} and higher, and then equating coefficients. It is natural to require

that $|n_b + 1/s - n_a| < 1$, so that the maximal powers of the two sums in (4.6) are adjacent. If one chooses $n_a + n_b + 2 = n_N + 1$, then, for each cutoff length n_N , the integers n_a and n_b are uniquely determined from a linear system of equations. The prize we pay is that the so obtained coefficients depend on the cutoff n_N . One can now study convergence of the coefficients a_j and b_j , with respect to increasing values of n_N , or various quantities derived from a_j and b_j . Note that the leading coefficients a_0 and b_0 determine the prefactors as in (3.18). The resummed expression can also be used to compute zeros, inside or outside the radius of convergence of the cycle expansion $\sum h_j z^j$.

The scheme outlined in this section tacitly assumes that a representation of the form (4.3) holds in a disc of radius 1 around $z = 1$. Convergence is improved further if additional information about the asymptotics of sums like (4.2) is used in the ansatz (4.5).

4.2. Analytical continuation by integral transformations

We will now introduce a method which provides an analytic continuation of sums of the form (4.2) without relying on the ansatz (4.5).^{12),13)} The main idea is to rewrite the sum (4.2) as a sum over integrals with the help of Poisson summation and find an analytic continuation of each integral by contour deformation. In order to do so, we need to know the n dependence of the coefficients $h_n \equiv h(n)$ explicitly for all n . If the coefficients are not known analytically, one may proceed by approximating the large n behavior in the form

$$h(n) = n^{-1/s-1}(C_1 + C_2 n^{-1} + \dots), \quad n \neq 0,$$

and determine the constants C_i numerically from periodic orbit data. By using the Poisson resummation identity

$$\sum_{n=-\infty}^{\infty} \delta(x - n) = \sum_{m=-\infty}^{\infty} \exp(2\pi i m x), \quad (4.7)$$

we may write the sum (4.2) as

$$f(z) = \frac{1}{2}h(0) + \sum_{m=-\infty}^{\infty} \int_0^{\infty} dx e^{2\pi i m x} h(x) z^x. \quad (4.8)$$

The continuous variable x corresponds to the discrete summation index n and it is convenient to write $z = r \exp(i\sigma)$ from now on. The integrals are of course still not convergent for $r > 0$. An analytic continuation can be found by considering the contour integral, where the contour goes out along the real axis, makes a quarter circle to either the positive or negative imaginary axis and goes back to zero. By letting the radius of the circle go to infinity, we essentially rotate the line of integration from the real onto the imaginary axis. For the $m = 0$ term in (4.8), we transform $x \rightarrow ix$ and the integral takes on the form

$$\int_0^{\infty} dx h(x) r^x e^{ix\sigma} = i \int_0^{\infty} dx h(ix) r^{ix} e^{-x\sigma}.$$

The integrand is now exponentially decreasing for all $r > 0$ and $\sigma \neq 0$ or 2π . The last condition reminds us again of the existence of a branch cut at $\operatorname{Re} z \geq 1$. By the same technique, we find the analytic continuation for all the other integrals in (4.8). The real axis is then rotated according to $x \rightarrow \pm ix$ where \pm sign refers to the sign of m ,

$$\int_0^\infty dx e^{\pm 2\pi i |m|x} h(x) r^x e^{ix\sigma} = \pm i \int_0^\infty dx h(\pm ix) r^{\pm ix} e^{-x(2\pi|m|\pm\sigma)}.$$

Changing summation and integration, we can carry out the sum over $|m|$ explicitly and one finally obtains the standard formula

$$\begin{aligned} f(z) &= \frac{1}{2}h(0) + i \int_0^\infty dx h(ix) r^{ix} e^{-x\sigma} \\ &+ i \int_0^\infty dx \frac{e^{-2\pi x}}{1 - e^{-2\pi x}} [h(ix)r^{ix}e^{-x\sigma} - h(-ix)r^{-ix}e^{x\sigma}]. \end{aligned} \quad (4.9)$$

The transformation from the original sum to the two integrals in (4.9) is exact for $r \leq 1$, and provides an analytic continuation for $r > 0$. The expression (4.9) is especially useful for an efficient numerical calculations of the dynamical zeta function for $|z| > 1$, which is essential when searching for zeros and poles of the zeta function.

4.3. Curvature contributions

So far, we have discussed the fundamental term $\sum_{n=1}^\infty t_n$ in (4.1) and showed ways to extract the information from such power series with algebraically decreasing coefficients. The fundamental term determines the main structure of the zeta function in terms of the leading order branch cut. Corrections to both the zeros and poles of the dynamical zeta function as well as the leading and sub-leading order terms in expansions like (4.3) are contained in the curvature terms in (4.1). The first curvature correction

$$\sum_{k=1}^\infty \sum_{m=1}^\infty \frac{1}{2} (t_{km} - t_k t_m)$$

also has algebraically decaying coefficients which diverge for $|z| > 1$. The analytically continued curvature terms have again branch cuts along the positive real z -axis. Our ability to calculate the higher order curvature terms depends on how much we know about the cycle weights t_{km} . The cycle expansion itself suggests that the terms t_{km} decrease asymptotically like

$$t_{km} \sim \frac{1}{(km)^{1+1/s}} \quad (4.10)$$

for 2-cycles of the induced map and in general for n -cycles like

$$t_{m_1 m_2 \dots m_n} \sim \frac{1}{(m_1 m_2 \dots m_n)^{1+1/s}}.$$

If we know the cycle weights $t_{m_1 m_2 \dots m_n}$ analytically, we may proceed like in §4.2 by transforming the multiple sums into multiple integrals and by rotating the axis' of integration.

§5. Summary and conclusions

Marginally stable orbits affect the analytic structure of dynamical zeta functions and the rules for constructing cycle expansions: While the marginal orbits have to be omitted, the cycle expansions need to include families of infinitely many longer and longer unstable orbits which accumulate towards the marginally stable cycles. Correlations for such non-hyperbolic systems decay algebraically with the decay rates controlled by the branch cuts of dynamical zeta functions. Compared to pure hyperbolic systems, the physical consequences are drastic: exponential decays are replaced by slow power law decays, and transport properties, such as the diffusion, may become anomalous.^{40),41)}

Acknowledgements

The authors are grateful to P. Dählqvist for his key contributions to this work and to the “Intermittency” chapter of Ref. 17), and to T. Prellberg for critical comments. G. T. and R. A. thank the Center for Nonlinear Science for hospitality at Georgia Tech, where part of the work was done with support by Glen P. Robinson Chair. R. A. was partially supported by the PRIN-2000 project “Chaos and localization in classical and quantum systems”, by INFN PA “Weak chaos: theory and applications”, and by EU contract QTRANS Network (“Quantum transport on an atomic scale”). G. T. acknowledges support by the Nuffield foundation, the EPSRC and the Royal Society.

References

- 1) P. Manneville and Y. Pomeau, *Phys. Lett. A* **75** (1979), 1.
- 2) Y. Pomeau and P. Manneville, *Commun. Math. Phys.* **74** (1980), 189.
- 3) R. S. MacKay and J. D. Miess, *Hamiltonian Dynamical Systems* (Adam Hilger, Bristol, 1987).
- 4) D. H. Mayer, *Bull. Soc. Math. France* **104** (1976), 195.
- 5) D. Mayer and G. Roepstorff, *J. Stat. Phys.* **47** (1987), 149.
- 6) R. Artuso, P. Cvitanović and B. G. Kenny, *Phys. Rev. A* **39** (1989), 268.
- 7) P. Cvitanović, in *Non-linear Evolution and Chaotic Phenomena*, ed. P. Zweifel, G. Gallavotti and M. Anile (Plenum, New York 1987), p. 349.
- 8) P. Cvitanović, in *Number Theory and Physics, Les Houches 1989 Spring School*, ed. C. Itzykson, P. Moussa and M. Waldschmidt (Springer, New York, 1992).
- 9) R. Artuso, E. Aurell and P. Cvitanović, *Nonlinearity* **3** (1990), 361.
- 10) D. H. Mayer, *Ergodic Theory, Symbolic Dynamics and Hyperbolic Spaces*, ed. T. Bedford, M. Keane and C. Series (Oxford University Press, Oxford, 1991).
- 11) P. Cvitanović, K. Hansen, J. Rolf and G. Vattay, *Nonlinearity* **11** (1998), 1209.
- 12) G. Tanner and D. Wintgen, *Phys. Rev. Lett.* **75** (1995), 2928.
- 13) G. Tanner, K. T. Hansen and J. Main, *Nonlinearity* **9** (1996), 1641.
- 14) G. Tanner, *J. of Phys. A* **30** (1997), 2863.
- 15) D. Ruelle, *Statistical Mechanics, Thermodynamic Formalism* (Addison-Wesley, Reading MA, 1978).
- 16) P. Gaspard, *Chaos, Scattering and Statistical Mechanics* (Cambridge Univ. Press, Cambridge, 1997).
- 17) P. Cvitanović, R. Artuso, P. Dählqvist, R. Mainieri, G. Tanner, G. Vattay, N. Whelan and A. Wirzba, *Chaos: Classical and Quantum* (www.nbi.dk/ChaosBook/ 2003)
- 18) H. H. Rugh, *Nonlinearity* **5** (1992), 1237.

- 19) P. Cvitanović, P. E. Rosenqvist, H. H. Rugh and G. Vattay, *Chaos* **3** (1993), 619.
- 20) C. P. Dettmann and P. Cvitanović, *Phys. Rev. E* **56** (1997), 6687; “Stability ordering of cycle expansions” section of Ref. 17).
- 21) P. Dahlqvist, *J. of Phys. A* **27** (1994), 763.
- 22) P. Dahlqvist, *Nonlinearity* **8** (1995), 11.
- 23) P. Cvitanović, *Phys. Rev. Lett.* **61** (1988), 2729.
- 24) R. Artuso, E. Aurell and P. Cvitanović, *Nonlinearity* **3** (1990), 325.
- 25) H. H. Rugh, *Inv. Math.* **135** (1999), 1.
- 26) S. Isola, *J. Stat. Phys.* **97** (1999), 263.
- 27) S. Isola, *Nonlinearity* **15** (2002), 1521.
- 28) T. Prellberg, nlin.CD/0108044.
- 29) T. Prellberg, *Maps of the interval with indifferent fixed points: thermodynamic formalism and phase transitions*, Ph.D. Thesis (Virginia Polytechnic Inst., 1991).
- 30) T. Prellberg and J. Slawny, *J. Stat. Phys.* **66** (1992), 503.
- 31) P. Gaspard and X.-J. Wang, *Proc. Natl. Acad. Sci. U.S.A.* **85** (1988), 4591.
X.-J. Wang, *Phys. Rev. A* **40** (1989), 6647; *Phys. Rev. A* **39** (1989), 3214.
- 32) B. Fornberg and K. S. Kölbig, *Math. of Computation* **29** (1975), 582.
- 33) A. Erdélyi, W. Magnus, F. Oberhettinger and F. G. Tricomi, *Higher transcendental functions, Vol. I* (McGraw-Hill, New York, 1953).
- 34) The proof of the bound (3.14) can be found in P. Dahlqvist’s unpublished notes, www.nbi.dk/ChaosBook/extras/PDahlqvistEscape.ps.gz.
- 35) Z. Kaufmann, H. Lustfeld and J. Bene, *Phys. Rev. E* **53** (1996), 1416.
- 36) P. Dahlqvist, *J. of Phys. A* **30** (1997), L351.
- 37) S. F. Nielsen, P. Dahlqvist and P. Cvitanović, *J. of Phys. A* **32** (1999), 6757.
- 38) P. Dahlqvist, *Phys. Rev. E* **60** (1999), 6639.
- 39) For an introduction to Tauberian theorems for power series and Laplace transforms see: W. Feller, *An introduction to probability theory and applications, Vol. II* (Wiley, New York, 1966).
- 40) R. Artuso, G. Casati and R. Lombardi, *Phys. Rev. Lett.* **71** (1993), 62.
- 41) Section *Marginal stability and anomalous diffusion*, Ref. 17).